MEDWIN PUBLISHERS
Committed to Create Value for Researchers

Medicinal and Analytical Chemistry International Journal
ISSN: 2639-2534

A Voltammetric Biosensor Based on Glassy Carbon Electrode Modified with DsDNA/ZIF-8/CNT for Determination of Malathion

Beigmoradi F[1], Masoud RM[1]*, Bazmandegan-Shamili A[1], Garkani-Nejad Z[2] and Nozohour-Yazdi M[3]

[1]Department of Chemistry, Vali-e-Asr University of Rafsanjan, Iran
[2]Department of Chemistry, Shahid Bahonar University of Kerman, Iran
[3]Department of Chemistry, Yazd University, Iran

Research Article
Volume 7 Issue 2
Received Date: August 09, 2023
Published Date: December 08, 2023
DOI: 10.23880/macij-16000182

***Corresponding author:** Masoud Rohani Moghadam, Department of Chemistry, Faculty of Sciences, Vali-e-Asr University of Rafsanjan, Rafsanjan, Iran, Email: masoud.rohani.moghadam@gmail.com; m.rohani@vru.ac.ir

Abstract

In this work, we constructed an electrochemical biosensor based on a glassy carbon electrode modified by dsDNA/ZIF-8/CNT for sensitive and selective measurement of malathion (MAL). First, we investigated the interaction between MAL and salmon sperm dsDNA by computational (molecular docking) and experimental (UV-visible spectroscopy, and electrochemistry) methods. Then, we prepared the ZIF-8/CNT sensor and immobilized dsDNA on it. The ZIF-8/CNT was characterized by fourier transform infrared spectroscopy, X-ray scattering spectroscopy, and field-emission scanning electron microscopy. We optimized the factors affecting the electrochemical response of MAL and immobilization of the dsDNA on the surface of ZIF-8/CNT/GCE, such as microliter of ZIF-8/CNT, concentration of the dsDNA and the time required for immobilization of dsDNA on the surface of ZIF-8/CNT-GCE, the effect of buffer pH on the MAL accumulation, the effect of MAL accumulation time, and the effect of pH the measurement solution. After optimizing the effective parameters, we drew the calibration curve using the differential pulse voltammetry (DPV) technique and obtained the concentration range of 0.20-50.00 µM with a detection limit of 1.0 nM. Furthermore, the RSD% for five consecutive tests of 2.00 µM MAL was obtained 2.4%. Also, the dsDNA/ZIF-8/CNT sensor showed good recovery in fruit samples.

Keywords: Glassy Carbon Electrode; Salmon Sperm Dsdna; Malathion; Zif-8/Cnt; Molecular Docking

Abbreviations

MAL: Malathion; HPLC: High Performance Liquid Chromatography; GC: Gas Chromatography; CE: Capillary Electrophoresis; IUPAC: International Union of Pure and Applied Chemistry; dsDNA: double-stranded Deoxyribo Nucleic Acid; MD: Molecular Docking; ZIFs: Zeolite Frameworks Based on Imidazole; CNTs: Carbon Nanotubes; GO: Graphene Oxide; GCE: Glassy Carbon Electrode; SWCNTs: Single-Wall Carbon Nanotubes; CPF: Chlorpyrifos; DZN: Diazinon; DLM: Deltamethrin; FNT: Fenitrothion; SDS: Sodium Dodecyl Sulfate; COD: Crystallography Open Database; DG: Deoxyguanosine; DPV: Differential Pulse Voltammetry; EIS: Electrochemical Impedance Spectroscopy; CV: Cyclic Voltammetry.

Introduction

The use of pesticides in agriculture has been one of the most important factors in increasing yield and reducing production costs. Organophosphorus pesticides are among the most common pesticides in the world. Malathion (S-1,2-bis(ethoxy carbonyl) ethyl O,O-dimethyl phosphorodithionate) (MAL) is a non-systemic insecticide, classified as a Class III Carcinogenic substances by the EPA [1]. The mechanism of organophosphorus pesticides such as MAL is the effect on the activity of the acetylcholinesterase enzyme and the accumulation of acetylcholine in the nerve terminals, which causes disturbances in the central nervous system and is considered a serious threat to human health [2]. Therefore, its measurement is very important. So far, various methods such as high performance liquid chromatography (HPLC) [3], gas chromatography (GC) [4], capillary electrophoresis (CE) [5], colorimetry [6], and electrochemical methods [7] have been reported for the measurement of MAL. Among the reported methods, electrochemical methods have received much attention due to having advantages such as high sensitivity and selectivity, low detection limit, fast response, low analyte consumption, and wide analyte range [8-10].

The International Union of Pure and Applied Chemistry (IUPAC) defined biosensors as devices that can provide quantitative information from a combination of bioreceptors and transducers that are directly connected to each other [11]. In double-stranded deoxyribonucleic acid (dsDNA) biosensors, dsDNA is used as a biological receptor.

The interaction between DNA and small molecules such as pesticides can be divided into intercalation, groove binding and electrostatic interactions [12]. Experimental methods such as electrochemical methods, UV-visible spectroscopy and computational methods such as molecular docking, etc have been used to investigate the interaction between DNA and small molecules (pesticides) [13-16]. Molecular docking (MD) is a computational method based on different orientations between ligand and monomer, scoring and calculating the binding energy of different modes based on software algorithms and determining the most favorable complex formed with the lowest energy level [17,18].

Immobilization of dsDNA is important for the construction of DNA biosensors [19]. Nanomaterials increase the surface of the electrode and as a result increase the sensitivity and signal of the biosensor. Metal-organic frameworks are crystalline compounds and contain metal ions or clusters that are often attached to organic molecules as connectors. Such multiple connections create one, two, or three dimensional structures, which can also be porous [20]. An interesting family of MOFs is zeolite frameworks based on imidazole (ZIFs). ZIFs are an important class of metal-organic frameworks that contain inorganic zinc ions that act as 2-methylimidazole-linked nodes [21]. ZIFs have properties such as special cross-sectional area, flexible cavities, thermal stability and stability in acidic conditions [22]. Among the ZIF materials, ZIF-8 has been widely used because it is compatible with carbon nanotubes (CNTs), polymers, graphene oxide (GO), etc [23-25]. ZIF-8 has applications in the fields of gas adsorption, selective separation, drug release, catalysis, sensors, and medical imaging [26]. The integration of ZIF-8 with CNT increases the conductivity and the electron transfer, which eliminates the limitation of low conductivity of ZIF-8 and also increases the surface area [10, 27]. On the other hand, the presence of carboxylic and amine groups of ZIF-8/CNT causes better dsDNA binding, and also ZIF-8/CNT has good biocompatibility properties, for this reason it is used in the manufacture of biosensors [27, 28]. Having a favorable interaction of dsDNA with MAL (computational and experimental methods) allows its detection and measurement.

In this paper, a simple and sensitive electrochemical biosensor was prepared to measure MAL. For this purpose, UV-Vis spectroscopic and electrochemical methods, also molecular binding calculations were used to investigate the interaction between dsDNA and MAL. Then, ZIF-8/CNT was synthesized. In the next step, the glassy carbon electrode (GCE) was modified with ZIF-8/CNT and dsDNA immobilized on the ZIF-8/CNT/GCE and was applied for the determination of MAL in fruit samples.

Materials and Methods

Single-wall carbon nanotubes (SWCNTs) (>98%; inner diameter: 0.8–1.6 nm; outer diameter: 1–2 nm; length: 30 μm), dsDNA, MAL, chlorpyrifos (CPF), diazinon (DZN), deltamethrin (DLM), and fenitrothion (FNT) were purchased from Sigma-Aldrich (Steinheim, Germany). Sodium dodecyl sulfate (SDS), 2-Methylimidazole (2-MeIm), methanol, ethanol, zinc nitrate hexahydrate, H3PO4, and NaOH were purchased from Merck (Darmstadt, Germany). A standard stock solution of MAL was prepared at 0.01 mol L-1 acetic acid. All solutions were prepared by dilution of the necessary amount of stock solution with water purified by a Milli-Q Gradient System A10 (Millipore, USA). Several phosphate buffer solutions in the pH range of 4.0 to 10.0 were prepared from 0.1 mol L-1 H3PO4 and 0.1 mol L-1 NaOH. Before performing the electrochemical tests, the nitrogen gas was purged in the solution for five minutes. Fresh fruit samples were purchased from regional supermarkets in Rafsanjan, a city in Kerman province.

Instrumentation

All electrochemical analysis were performed by Autolab Metrohm PGSTAT204 (Switzerland, www.metrohm.com) in a three-electrode system containing an Ag/AgCl as the reference electrode, a platinum wire as the auxiliary electrode, and the glassy carbon electrode as the working electrode. The pH measurements were done by a Metrohm 827 pH meter (Switzerland, www.metrohm.com) with combined glass-calomel electrode. The FT-IR and the X-ray analysis were taken by the Thermo Fisher Scientific (Nicolet is10, USA) FT-IR and X' Pert Pro instruments (Panalytical, Iran, https://iranindustryexpo.com), respectively. The UV–visible analysis was performed by a CARY 100 Conc UV-Visible spectrophotometer. Also, the morphology and Energy-dispersive X-ray spectroscopy (EDX) were taken by field emission scanning electron microscope (FE-SEM) Zeiss Sigma-VP FESEM instrument (Jena, Germany, http://www.zeiss.com).

Synthesis of ZIF-8/CNT

ZIF-8/CNT was synthesized using the method of Zheng, et al. [29] with minor modifications. First, 0.1 g of SDS was dissolved in 20 mL of ethanol and stirred for 5 minutes. Then, 15.00 mg of CNT and 0.24 g of 2-MeIm were added to the solution and stirred for 24 hours (solution 1). Next, 0.28 g of zinc nitrate hexahydrate was dissolved in 20 mL of methanol to form solution 2. Solution 2 was added to solution 1 and stirred for 5 minutes. The final solution was kept at room temperature for 24 hours. ZIF-8/CNT was washed several times with methanol and dried at 60°C.

Preparation of the ZIF-8/CNT Glassy Carbon Electrode

1 mg of ZIF-8/CNT was poured into a microtube and 1 ml of distilled water was added. The microtube was placed in an ultrasonic bath for 10 minutes to homogenize the ZIF-8/CNT. The GCE electrode was polished with alumina suspension. 4 µl of ZIF-8/CNT solution was taken on the GCE electrode and the electrode was allowed to dry for 15 minutes.

Preparation of the ZIF-8/CNT/dsDNA Glassy Carbon Electrode

The dsDNA was immobilized on the GCE surface modified with ZIF-8/CNT according to the method of Mahmoudi-Moghaddam, et al. [30] with a slight modification. The desired electrode was placed in 25 ml of a solution containing 0.5 M acetate buffer with pH = 4.8, which contains 150 µM dsDNA. The potential of 0.5 V was applied to the stirring solution for 200 seconds. The electrode was washed with acetate buffer.

Preparation of Vegetable Samples

The edible parts of the cucumbers and lettuces were washed with ultrapure water, dried for 24 hours at room temperature, and vegetable juice was extracted. 10 ml of vegetable juice was mixed with 1 ml of 0.01 M acetic acid and centrifuged at 8000 rpm for 15 minutes. The liquid phase was used for MAL determination and stored at 4 °C if not used. Specific amounts of MAL were added to the liquid phase to test the recovery.

Results and Discussion

Characterization Studies

FT-IR Studies: FT-IR spectra of CNT (a), ZIF-8 (b) and ZIF-8/CNT (c) are shown in Figure 1. As the figure shows, the absorption band from frequency 3200 to 1350 cm-1 indicates N-H stretching vibrations. The C-N stretching vibration appears in the frequency range of 995 and 1141 cm-1. The stretching vibration C=N of the benzene ring appears at the frequency of 1587 cm-1. In addition, C-H stretching vibration is seen at 2848 and 2914 cm-1 frequencies.

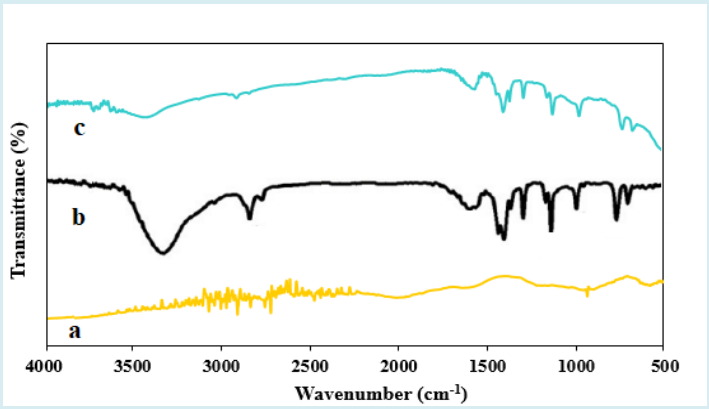

Figure 1: Fourier transform infrared (FT-IR) spectra of CNT (a), ZIF-8 (b), and ZIF-8/CNT (c).

FESEM Studies

The morphology of ZIF-8/CNT at two different scales is shown in Figure 2A and 2B. As shows, the morphology of ZIF-8 is hexagonal. In addition, CNTs enter the ZIF-8 crystals from different directions, while the crystal structure of ZIF-8 is preserved.

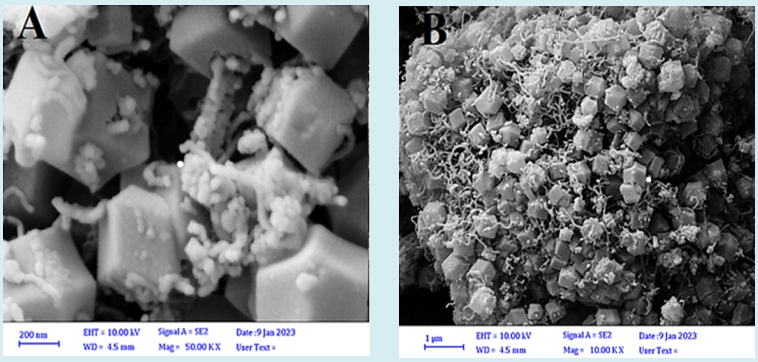

Figure 2: Field emission scanning electron microscopy (FESEM) images of ZIF-8/CNT in different dimensions: 200 nm (A) and 1 µm (B).

EDS Studies

The EDS spectrum of ZIF-8/CNT (Figure 3) shows all the main elements of the structure, including nitrogen (N), zinc (Zn), carbon (C), and oxygen (O). The presence of these elements confirms the formation of the desired ZIF-8. The weight percentage of each element is shown in the attachment to each spectrum. The weight percentage of nitrogen in ZIF-8/CNT is 9.6%, which is consistent with the expected value for ZIF-8. The weight percentage of zinc in ZIF-8/CNT is 29.8%, which is also consistent with the expected value for ZIF-8. The weight percentage of carbon in ZIF-8/CNT is 56.2%, which is slightly higher than the expected value for ZIF-8. This is likely due to the presence of CNTs in the sample.

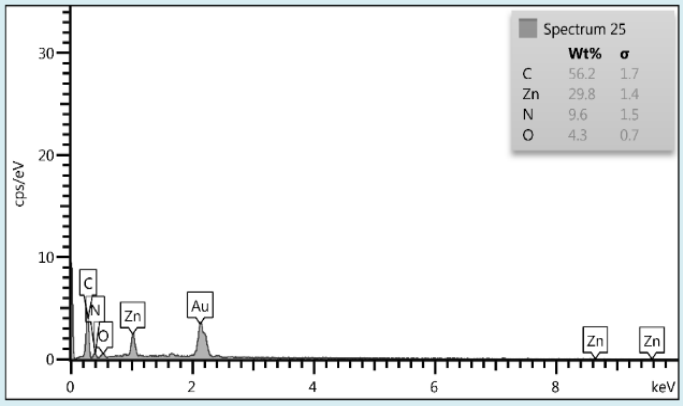

Figure 3: Energy-dispersive X-ray spectroscopy (EDS) spectrum of ZIF-8/CNT.

XRD Studies

The XRD pattern of ZIF-8 (Figure S1a) shows sharp peaks at 2θ values of 7.39°, 10.47°, 12.81°, 14.81°, 16.50°, and 18.12°. These peaks correspond to the (0 1 1), (0 0 2), (1 1 2), (0 2 2), (0 1 3), and (2 2 2) planes, respectively. The presence of these peaks confirms the formation of ZIF-8. The XRD pattern of ZIF-8/CNT (Figure S1b) also shows sharp peaks at the same 2θ values as ZIF-8. This indicates that the crystalline structure of ZIF-8 was preserved after blending with CNT. The good crystallinity of ZIF-8 nanostructures is also evident from their relative intensities. The relative intensities of the peaks in the XRD pattern of ZIF-8/CNT are similar to those in the XRD pattern of ZIF-8. This indicates that the blending of ZIF-8 with CNT did not significantly affect the crystallinity of ZIF-8. Also, to confirm the desired synthesis, the PXRD ZIF-8 reference template of the Crystallography Open Database (COD) site was used, and the sharp peaks ZIF-8 of this reference confirm the successful synthesis of the present work [31].

Computational and Experimental Methods to Investigate the Interaction Between MAL and dsDNA

Molecular Docking: The output from molecular docking is shown in Figure S2. MAL interacted with the minor groove of dsDNA and formed six hydrogen bonds as a result of the interaction. Two hydrogen bonds involving oxygen from MAL were formed with nitrogen from deoxyguanosine (DG) 44 and DG 222. In addition, two more hydrogen bonds were formed from the interaction of oxygen from MAL with nitrogen from DG 222 and DG 223. Also, two hydrogen bonds were formed from the interaction of sulfur from MAL with two nitrogens from DG 223. The binding energy of MAL with minor groove dsDNA was found to be -3.08 kcal/mol.

UV-Vis Spectroscopy: Figure S3, shows the absorption spectrum of the interaction of 140.00 µM of dsDNA in the presence of different concentrations of MAL. As the figure shows, increasing the concentration of MAL (0.00, 5.00, 10.00, 15.00, and 20.00 µM) to the dsDNA solution decreased the absorption peak intensity of dsDNA at 260 nm. This indicates a strong interaction between MAL and dsDNA, which causes the formation of a complex between MAL and dsDNA.

Differential Pulse Voltammetry (DPV) Study of MAL on ZIF-8/CNT/GCE Surface

To investigate the immobilization of MAL on GCE electrodes modified with ZIF-8/CNT/dsDNA and ZIF-8/CNT were placed in a solution containing 2.00 µM MAL prepared in 0.10 M phosphate buffer with pH 7.0 (Figure S4, curve a and b). The solution was stirred for 9 minutes by a magnetic stirrer. At this stage, MAL accumulated on the electrode surface. The electrode was then washed with distilled water and transferred to the electrochemical cell containing 0.10 M phosphate buffer (pH 7.0). Finally, using the DPV technique, its voltammograms were recorded in the potential range of -0.1 to 0.5 V. The current of MAL in Figure 7, curve a, is increased compared to curve b, indicating that MAL is accumulated by surface adsorption on ZIF-8/CNT/dsDNA/GCE, through its strong interaction with dsDNA.

Investigating dsDNA Immobilization on ZIF-8/CNT/GCE Surface

Cyclic voltammetry (CV) and electrochemical impedance spectroscopy (EIS) techniques were used to investigate the immobilization of dsDNA. 1 mM ferricyanide solution was used in the potential range of -0.2 to 0.7 V with a scan rate of 100 mV/s. A pair of reversible CV peaks around 0.2 V can be seen in Figure S5A. When the electrode was modified with ZIF-8/CNT, the voltammogram current increased (Figure S5A, curve b). When dsDNA was immobilized on ZIF-8/CNT/GCE, the voltammogram current decreased (Figure S5A, curve c). This is due to the repulsion between the negative charge of dsDNA and ferricyanide, which prevents it from reaching the electrode surface and causes the current to decrease. This indicates the immobilization of dsDNA on the electrode surface. In addition, EIS technique was used to investigate dsDNA immobilization on the ZIF-8/CNT/GCE surface. As shown in Figure S5B, when the bare GCE electrode was modified with ZIF-8/CNT, the electron transfer resistance was greatly reduced (curve b). When dsDNA was immobilized on the ZIF-8/CNT modified GCE electrode, the amount of electron transfer resistance increased. Figure 4 shows a schematic of malathion oxidation mechanism on the ZIF-8/CNT/dsDNA-GCE surface.

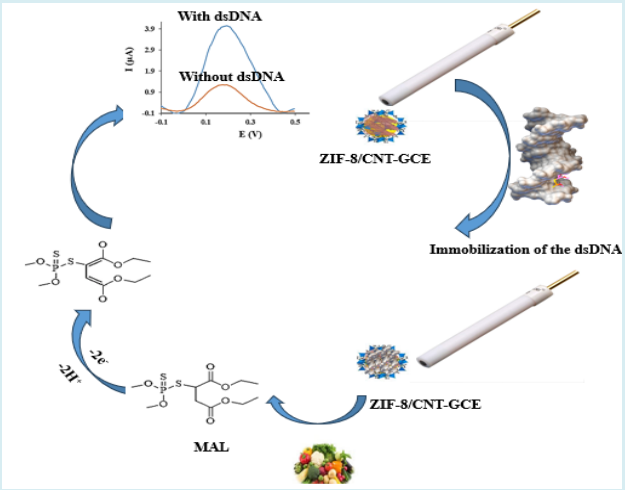

Figure 4: Schematic of the malathion oxidation mechanism of MAL at the ZIF-8/CNT/dsDNA-GCE surface.

Optimization of Parameters Affecting on the Electrochemical Response of ZIF-8/CNT/dsDNA/GCE Biosensor

The factors affecting the electrochemical response of MAL and immobilization of dsDNA on the surface of ZIF-8/CNT/GCE, such as the amount of ZIF-8/CNT, dsDNA concentration, time required to immobilize dsDNA on the surface of ZIF-8/CNT-GCE, buffer pH on MAL accumulation, MAL accumulation time, and pH of the measurement solution, were investigated and optimized. Different volumes of ZIF-8/CNT solution were used to modify the electrode surface and the other parameters were kept constant. As shown in Figure 5A, the current reached its maximum value when 6 µL of ZIF-8/CNT was used to modify the electrode surface. Therefore, 6 µL of ZIF-8/CNT was selected as the optimal amount. The concentration of dsDNA on the surface of ZIF-8/CNT-GCE plays a role in the electrochemical response of MAL. Therefore, different concentrations of dsDNA (10.0, 50.0, 100.0, 150.0, 200.0, and 250.0 µM) were selected. As Figure 5B shows, with the increase of dsDNA concentration up to 150.0 µM, the current reaches its maximum value and then the current decreases due to the saturation of the electrode surface. Therefore, the optimal dsDNA concentration was 150.0 µM. Figure 5C shows the effect of different times (100, 130, 160, 200, 220, and 250 seconds) on the electrochemical response of MAL. The best electrochemical response was obtained at 200 seconds and it was chosen as the optimal value. To optimize the pH of the phosphate buffer on the accumulation of MAL on the surface of ZIF-8/CNT/dsDNA-GCE, 0.1 M phosphate buffer in the pH range of 4.0 to 10.0 containing 25.0 µM MAL was used. As Figure 5D shows, when the pH increases from 4.0 to 7.0, the peak current of MAL also increases, and then the peak current of MAL decreases as the pH of the solution increases. Therefore, pH equal to 7.0 was selected as the optimal pH for MAL accumulation. The effect of MAL accumulation time on ZIF-8/CNT/dsDNA-GCE surface was also investigated. Figure 5E shows the effect of different MAL accumulation times (3, 5, 7, 9, 12, and 15 min). As Figure 5E shows, the maximum MAL current is achieved in 9 min. Therefore, 9 min was chosen as the optimal time for MAL accumulation. In order to obtain the best electrochemical response of MAL on ZIF-8/CNT/dsDNA-GCE surface, the pH effect of the measurement solution, 0.1 M phosphate buffer was made in the pH range of 4.0 to 10.0. As shown in Figure 5F, the highest current was obtained at pH 7.0 and decreased after that. Therefore, pH equal to 7.0 was chosen as the pH of the measuring solution Figure 5.

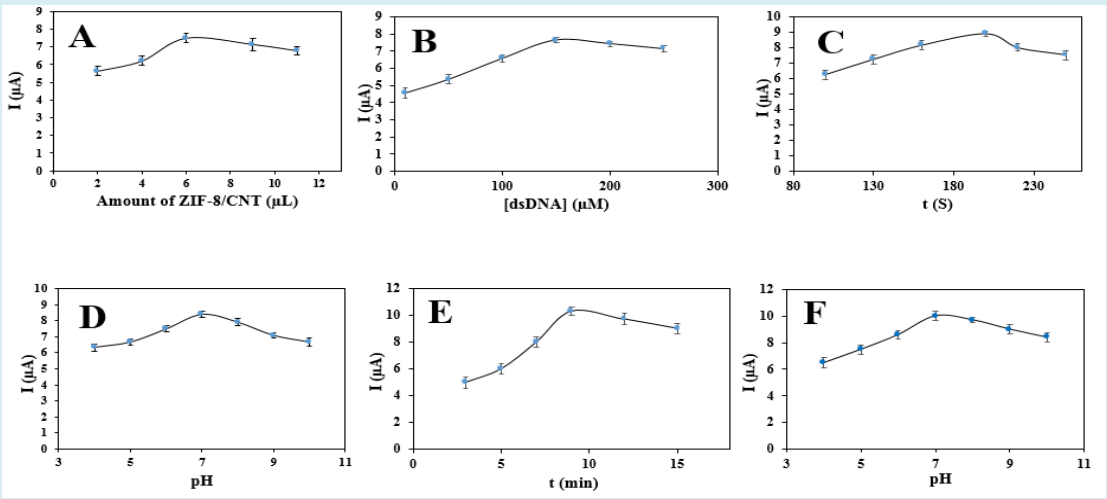

Figure 5: (A) Optimization of the volume of ZIF-8/CNT solution. Conditions: 8.00 µM MAL; dsDNA concentration, 200 µM; dsDNA immobilization time, 150 s; pH of extraction solution, 7.0; pH of measuring solution, 7.0; accumulation time: 7 min. (B) Optimization of the dsDNA concentration. Conditions: 8.00 µM MAL; volume of ZIF-8/CNT solution, 6 µM; dsDNA immobilization time, 150 s; pH of extraction solution, 7.0; pH of measuring solution, 7.0; accumulation time: 7 min. (C) Optimization of the dsDNA immobilization time. Conditions: 8.00 µM MAL; dsDNA concentration, 150 µM; volume of ZIF-8/CNT solution, 6 µM; pH of extraction solution, 7.0; pH of measuring solution, 7.0; accumulation time: 7 min. (D) Optimization of the pH of extraction solution. Conditions: 8.00 µM MAL; dsDNA concentration, 150 µM; volume of ZIF-8/CNT solution, 6 µM; dsDNA immobilization time, 200 s; pH of measuring solution, 7.0; accumulation time: 7 min. (E) Optimization of the MAL accumulation time. Conditions: 8.00 µM MAL; dsDNA concentration, 150 µM; volume of ZIF-8/CNT solution, 6 µM; dsDNA immobilization time, 200 s; pH of measuring solution, 7.0; pH of extraction solution, 7.0. (F) Optimization of the pH of measurement solution. Conditions: 8.00 µM MAL; dsDNA concentration, 150 µM; volume of ZIF-8/CNT solution, 6 µM; dsDNA immobilization time, 200 s; accumulation time: 9 min; pH of extraction solution, 7.0.

Studying the Properties of the ZIF-8/CNT/dsDNA-GCE Sensor on the Electrochemical Response of MAL

After investigating and optimizing the factors affecting the electrochemical response of MAL and dsDNA immobilization on the ZIF-8/CNT/GCE surface, a calibration curve was drawn under optimal conditions (Figure 6). As the figure shows, the peak current had a linear relationship with the MAL concentration in the concentration range of 0.20 to 50.00 µM. The equation of the line was y = 1.3009x + 4.637 (R2 = 0.9995). The limit of detection (LOD) was 1 nM with ten repetitions and the relative standard deviation (RSD) percentage was 2.4% for five consecutive experiments from the MAL concentration of 2.00 µM.

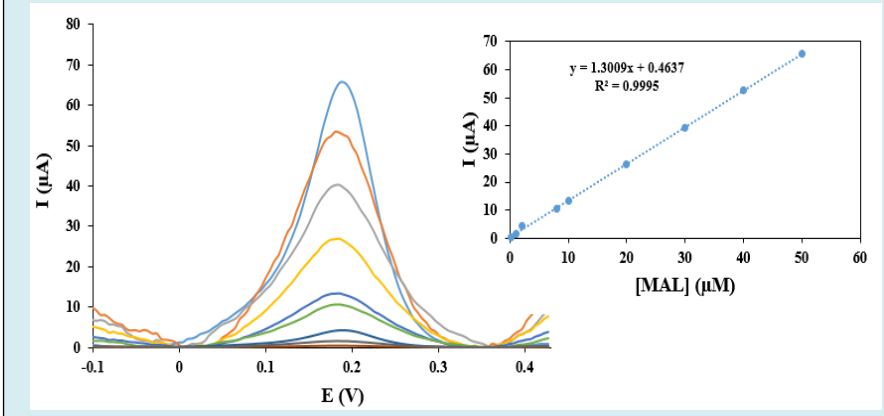

Figure 6: DPV curves of different concentrations from 0.20 to 50.00 µM MAL.

To check the stability of the biosensor, the ZIF-8/CNT/dsDNA-GCE sensor was used to measure 2.00 µM MAL solution every week. The measured current responses maintained 89.90 (±2.1) % of their initial value after seven weeks, indicating the stability of the ZIF-8/CNT/dsDNA-GCE sensor.

The selectivity of the ZIF-8/CNT/dsDNA-GCE sensor was also investigated with interfering species having a similar structure to MAL. Therefore, 2.00 µM MAL solution was selected in the presence of higher concentrations of CPF, DZN, DLM, and FNT. The tolerance limit was defined as the maximum interference concentration that provides less than ±5% relative error. The presence of interfering species has no effect on the MAL measurement at a given concentration, as shown in Table S1.

Measurement of Vegetable Samples

To evaluate the ability of the ZIF-8/CNT/dsDNA-GCE sensor in measuring MAL, the prepared sensor was used to measure MAL in cucumber and lettuce samples, and the results are listed in Table 1. The pH of the obtained solutions was adjusted to 7.0 with phosphate buffer. If the solution was not used immediately, it was stored at 4 °C and a certain amount of MAL was added to the liquid phase for the recovery experiment.

Sample	Spiked (µM)	Found (µM)	Recovery (%)
Cucumber juice	0	-	-
	11.5	11.7	101.7
	16.5	16.3	98.8
	21.5	21.9	101.9
Lettuce juice	0	-	-
	5.5	5.3	96.4
	7.5	7.7	102.6
	10.5	10.3	98.1

Table 1: Results of MAL determination in vegetable samples.

Comparison of ZIF-8/CNT/dsDNA-GCE Sensor Compared to Other Electrochemical Sensors

To compare the ZIF-8/CNT/dsDNA-GCE sensor with other electrochemical sensors for measuring MAL, a series of experiments were conducted. The results showed that the ZIF-8/CNT/dsDNA-GCE sensor had the lowest limit of detection (LOD) value of 1 nM, which was significantly lower than the LOD values of the other sensors (Table 2). In addition, the ZIF-8/CNT/dsDNA-GCE sensor also had a comparable response to the other sensors, indicating that it is a promising tool for the sensitive detection of MAL.

Modifier	Method	LOD	LDR	Ref
NH_2–Al MOF[a]	LSV	5.1 µM	3.0 µM-15.0 mM	[32]
PA6/PPy/CRGO[b]	DPV	2.4 nM	1.5-60.5 µM	[33]
AChE/PANI– PPY-MWCNTs[c]	CV	3.0 nM	0.03-1.5 and 3.0-75.0 µM	[34]
Aptamer/MOF-CP-Fc[d]/AuNPs	DPV	17.2 µM	25.0-850.0 µM	[35]
COF@MWCNT/ AChE[e]	DPV	0.5 µM	0.001-10.0 µM	[36]
ZIF-8/CNT/dsDNA	DPV	1.0 nM	0.2-50.0 µM	This work

Table 2: Comparison of ZIF-8/CNT/dsDNA-GCE with some recently reported electrochemical sensors.
[a]Aluminum MOF functionalized with amine. [b]Polyamide 6/polypyrrole electrospun nanofibers coated with reduced graphene oxide. [c]Acetylcholinesterase coated on Polyaniline and polypyrrole copolymer doped with multi-walled carbon nanotubs. [d]Metal organic framework complementary probe carboxy-ferrocene. [e]Covalent organic framework coated of Multi walled carbon nanotubes.

Conclusion

In this study, we developed a novel ZIF-8/CNT/dsDNA-GCE electrochemical sensor for the sensitive detection of MAL. The interaction between MAL and dsDNA was first studied using theoretical and experimental methods. The characterization of ZIF-8/CNT was then investigated by FT-IR, FESEM, EDS, and XRD measurements. The GCE electrode was then modified with ZIF-8/CNT and dsDNA was immobilized on it. The parameters affecting MAL electrochemical signal and dsDNA stabilization were optimized. The resulting sensor showed excellent performance, including easy preparation method, high selectivity, good reproducibility, linear range from 0.20 to 50.00 µM, detection limit of 1 nM, and successful determination of MAL in cucumber and lettuce samples.

Refrences

1. Kadam AN, Dhabbe RS, Kokate MR, Gaikwad YB, Garadkar KM (2014) Preparation of N doped TiO2 via microwave-assisted method and its photocatalytic activity for degradation of Malathion. Spectrochim Acta A Mol Biomol Spectrosc 133: 669-676.

2. He L, Cui B, Liu J, Song Y, Wang M, et al. (2018) Novel electrochemical biosensor based on core-shell nanostructured composite of hollow carbon spheres and polyaniline for sensitively detecting malathion. Sens Actuators B Chem 258: 813-821.

3. Markovska LV, Ilievska BP (2022) Determination of malathion and its residues by normal-phase high-performance liquid chromatography method. Acta Chromatogr 34(3): 315-322.

4. Yeganeh M, Azari A, Sobhi HR, Farzadkia M, Esrafili A, et al. (2021) A comprehensive systematic review and meta-analysis on the extraction of pesticide by various solid phase-based separation methods: a case study of malathion. Environ Anal Chem 103(5): 1068-1085.

5. Ruiz CG, Llamas GA, Puerta A, Blanco E, Medel AS, et al. (2005) Enantiomeric separation of organophosphorus pesticides by capillary electrophoresis: Application to the determination of malathion in water samples after preconcentration by off-line solid-phase extraction. Anal Chim acta 543(1-2): 77-83.

6. Sahu B, Kurrey R, Deb MK, Khalkho BR, Manikpuri S (2023) Recognition of malathion pesticides in agricultural samples by using α-CD functionalized gold nanoparticles as a colorimetric sensor. Talanta 259: 124526.

7. Beigmoradi F, Moghadam MR, Garkani-Nejad Z, Shamili AB, Masoodi HR (2023) Dual-template imprinted polymer electrochemical sensor for simultaneous de-termination of malathion and carbendazim using graphene quantum dots. Anal Methods 15(38).

8. Ermis N, Zare N, Darabi R, Alizadeh M, Karimi F, et al. (2023) Recent advantage in electrochemical monitoring

of gallic acid and kojic acid: A new perspective in food science. Food Meas Charact 17(4): 3644-3653.

9. Bilal S, Nasir M, Hassan MM, Sami AJ, Hayat A, et al. (2022) A novel construct of an electrochemical acetylcholinesterase biosensor for the investigation of malathion sensitivity to three different insect species using a NiCr2O4/gC3N4 composite integrated pencil graphite electrode. RSC advances 12(26): 16860-16874.

10. Oliveira RHD, Gonçalves DA, Reis DDD (2023) TiO2/MWCNT/Nafion-Modified Glassy Carbon Electrode as a Sensitive Voltammetric Sensor for the Determination of Hydrogen Peroxide. Sens 23(18): 7732.

11. Singh A, Sharma A, Ahmed A, Sundramoorthy AK, Furukawa H, et al. (2021) Recent advances in electrochemical biosensors: Applications, challenges, and future scope. Biosens 11(9): 336.

12. Almaqwashi AA, Paramanathan T, Rouzina I, Williams MC (2016) Mechanisms of small molecule-DNA interactions probed by single-molecule force spectroscopy. Nucleic acids Res 44(9): 3971-3988.

13. Temerk Y, Ibrahim H (2015) Electrochemical studies and spectroscopic investigations on the interaction of an anticancer drug flutamide with DNA and its analytical applications. Electroanal Chem 736: 1-7.

14. Morawska K, Popławski T, Ciesielski W, Smarzewska S (2020) Interactions of lamotrigine with single-and double-stranded DNA under physiological conditions. Bioelectrochemistry 136: 107630.

15. Morawska K, Jedlińska K, Smarzewska S, Metelka R, Ciesielski W, et al. (2019) Analysis and DNA interaction of the profluralin herbicide. Environ Chem Lett 17: 1359-1365.

16. Srivastava AK, Singh D (2020) Assessment of malathion toxicity on cytophysiological activity DNA damage and antioxidant enzymes in root of Allium cepa model. Sci Rep 10(1): 886.

17. Fan J, Fu A, Zhang L (2019) Progress in molecular docking. Quant Biol 7: 83-89.

18. Silva CF, Borges KB, Nascimento CS (2019) Computational study on acetamiprid-molecular imprinted polymer. Mol Model 25: 104.

19. Moghaddam HM, Nejad ZG (2022) A new electrochemical DNA biosensor for determination of anti-cancer drug chlorambucil based on a polypyrrole/flower-like platinum/NiCo2 O4/pencil graphite electrode. RSC Adv 12(8): 5001-5011.

20. Shanmugam R, Aniruthan S, Yamunadevi V, Nellaiappan S, Amali AJ, et al. (2023) Co-N/Zn@ NPC Derived from Bimetallic Zeolitic Imidazolate Frameworks: A Dual Mode Simultaneous Electrochemical Sensor for Uric Acid and Ascorbic Acid. Surf Interfaces 40: 103103.

21. Kwon O, Kim M, Choi E, Bae JH, Yoo S, et al. (2022) High-aspect ratio zeolitic imidazolate framework (ZIF) nanoplates for hydrocarbon separation membranes. Sci Adv 8(1): eabl6841.

22. Ahmad I, Muhmood T, Rehman A, Zahid M, Abohashrh M, et al. (2023) Zeolite imidazole framework entrapped quantum dots (QDs@ ZIF-8): encapsulation properties and applications. Taiwan Inst Chem Eng 149: 104993.

23. Yan W, Zhou S, Ling M, Peng X, Zhou H (2022) NH3 Sensor Based on ZIF-8/CNT Operating at Room Temperature with Immunity to Humidity. Inorganics 10(11): 193.

24. Li W, Lin Z, Zuo H, Zhong J, Xu Y, et al. (2022) ZIF-8@ Co-doped boronate ester polymer core-shell particles: Catalytically enhancing the nonflammability and smoke suppression of epoxy resin. Poly Degrad Stab 198: 109877.

25. Wu X, Zhang H, Yin Z, Yang Y, Wang Z (2022) ZIF-8/GO sandwich composite membranes through a precursor conversion strategy for H2/CO2 separation. Membr Sci 647: 120291.

26. Ahmadi M, Khoramjouy M, Dadashzadeh S, Asadian E, Mosayebnia M, et al. (2023) Pharmacokinetics and biodistribution studies of [99mTc]-Labeled ZIF-8 nanoparticles to pave the way for image-guided drug delivery and theranostics. Drug Deliv Sci Technol 81: 104249.

27. Chronopoulos DD, Saini H, Tantis I, Zbořil R, Jayaramulu K, et al. (2022) Carbon nanotube based metal-organic framework hybrids from fundamentals toward applications. Small 18(4): 2104628.

28. Ren Q, Mou J, Guo Y, Wang H, Cao X, et al. (2020) Simple homogeneous electrochemical target-responsive aptasensor based on aptamer bio-gated and porous carbon nanocontainer derived from ZIF-8. Biosens Bioelectron 166: 112448.

29. Fu F, Zheng B, Xie LH, Du H, Du S, et al. (2018) Size-controllable synthesis of zeolitic imidazolate framework/carbon nanotube composites. Crystals 8(10): 367.

30. Moghaddam HM, Tajik S, Beitollahi H (2019) A new electrochemical DNA biosensor based on modified carbon paste electrode using graphene quantum

dots and ionic liquid for determination of topotecan. Microchem 150: 104085.

31. Karagiaridi O, Lalonde MB, Bury W, Sarjeant AA, Farha OK, et al. (2012) Opening ZIF-8: a catalytically active zeolitic imidazolate framework of sodalite topology with unsubstituted linkers. Am Cheml Soc 134(45): 18790-18796.

32. Nikhar S, Kumar P (2022) Electrochemical sensing of malathion using doped MOFs. IOP Conf Ser Mater Sci Eng 1225(1): 012055.

33. Migliorini FL, Sanfelice RC, Mercante LA, Facure MH, Correa DS (2019) Electrochemical sensor based on polyamide 6/polypyrrole electrospun nanofibers coated with reduced graphene oxide for malathion pesticide detection. Mater Res Express 7(1): 015601.

34. Du D, Ye X, Cai J, Liu J, Zhang A (2010) Acetylcholinesterase biosensor design based on carbon nanotube-encapsulated polypyrrole and polyaniline copolymer for amperometric detection of organophosphates. Biosen Bioelectron 25(11): 2503-2508.

35. Xu G, Huo D, Hou J, Zhang C, Zhao Y, et al. (2021) An electrochemical aptasensor of malathion based on ferrocene/DNA-hybridized MOF DNA coupling-gold nanoparticles and competitive DNA strand reaction. Microchem 162: 105829.

36. Wang X, Yang S, Shan J, Bai X (2022) Novel electrochemical acetylcholinesterase biosensor based on core-shell covalent organic framework@ multi-walled carbon nanotubes (COF@ MWCNTs) composite for detection of malathion. Electrochem Sci 17(5): 220543.